Chapter 6

Evaluation of a PV-driven innovative solar dryer for *Curcuma amada* without and with gravels as thermal energy storage: An investigation on kinetics, energy, exergy, quality and economic aspects

The chapter focuses on assessing the effectiveness of a PV-driven innovative solar dryer for the dehydration of *Curcuma amada*. It explores into several key areas, including the drying kinetics of *Curcuma amada* within the solar dryer, the energy efficiency of the solar air collector and dryer system, both with and without the utilization of thermal energy storage via gravels. Additionally, it conducts an exergy analysis to assess input, output, losses, and efficiency of the solar air collector and dryer, as well as a quality evaluation of the dehydrated *Curcuma amada*, covering total polyphenol and flavonoid content and color variations. Furthermore, the study includes an economic analysis examining the payback period and life cycle savings for various configurations of the solar dryer, with particular attention to the integration of thermal energy storage using storage. The study investigated the drying process *of Curcuma amada* to evaluate the suitability and efficiency of the dryer for another product. The idea is to check the practical implications and variability of the dryer. Furthermore, both *Garcinia pedunculata* and *Curcuma amada* are subject to seasonal availability. Modifying the system to accommodate crops available throughout the year facilitates continuous operation, maximizing its usage and advantages.

6.1 Development and experimentation

A photograph and a schematic of the experimental setup are given in Figure 6.1 and Figure 6.2 respectively. The system includes SAC, drying cabinet, DC fan, and solar panel. The SAC is a pivotal component within the solar drying system that emerges as a nexus of energy harvesting and efficiency. Waste beverage cans were used to enhance the heat transfer of the absorbent plate. Cans were coated with black paint to maximize heat absorption. In addition, a transparent cover was used to retain the sun's rays, by creating a greenhouse effect. Filled with gravels as sensible heat storage (SHS) material, the collector stores thermal energy during ample sunlight and releases it when energy is needed. This stored heat fuels two crucial functions: naturally heating the air within the collector through convection and facilitating controlled airflow through a strategically placed DC fan. The DC-motor fan at the bottom of a dryer had significantly enhanced the drying process through

forced convection. The fan facilitates improved air circulation and heat distribution within the drying chamber, ensuring that the heated air effectively reaches almost all parts of the material. This enhanced airflow promotes faster drying rates, contributing to more uniform moisture removal. The controlled movement of air also aids in temperature regulation, optimizing drying conditions for the specific material being processed. Additionally, the fan helps to prevent the formation of stagnant air pockets, which may hinder the drying efficiency. These benefits lead to increased energy efficiency and reduction in drying times. However, the DC fan's position is at the bottom center of the dryer, and hence the hot air flow pattern may not be uniform in all portions of the drying chamber (near the wall, hot air mass flow is lesser than at the center). The drying cabinet was made of stainless-steel sheet and a plywood cover insulation. Five perforated trays were employed to hold *Curcuma amada* during the drying process. The system incorporated a practical solution for year-round operation by utilizing an adjustable stand for the SAC. The experiments were conducted during March 2023. To evaluate the drying efficiency, two modes were considered: indirect solar drying integrated with canned absorber plate SAC but without SHS (SDCWOS) and the other is indirect solar drying integrated with canned absorber plate SAC with SHS (SDCWS). The trials were conducted from 8:30 to 16:30. Seven kilograms of fresh *Curcuma amada* were procured from the local market, cleansed, sliced, and placed in five trays within the improved solar dryer. Preceding the experiment, the dryer underwent a preheating period of one hour. In every operational setting, careful and precise drying procedures were conducted, considering the factors like solar radiation, surrounding temperature, temperatures at the inlet and outlet of the SAC and the dryer, as well as the product's weight loss. Each mode of experimentation was replicated six times under similar environmental conditions ensuring the reliability and accuracy of the results [20]. Table 6.1 gives specifications of the drying setup.

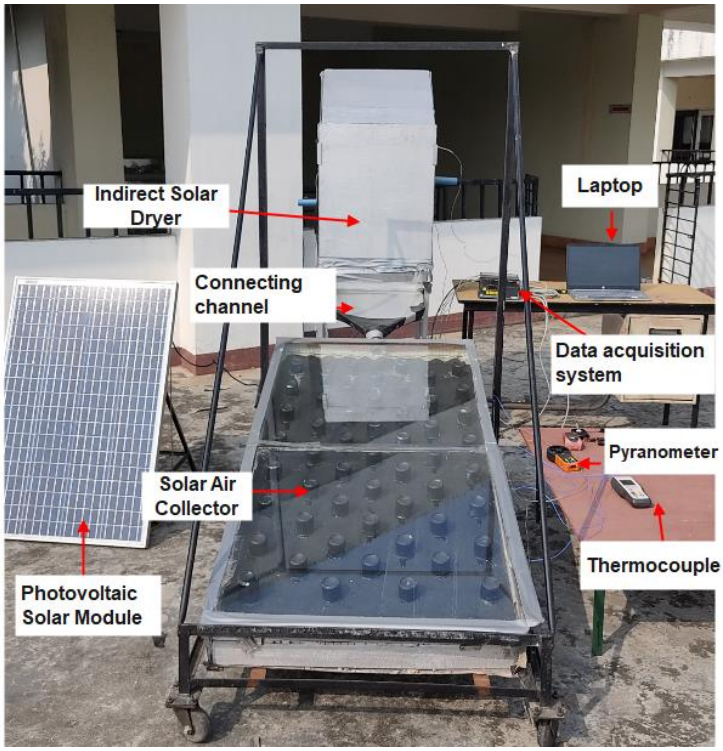

Figure 6.1 Photograph of the experimental set-up for drying of *Curcuma amada*.

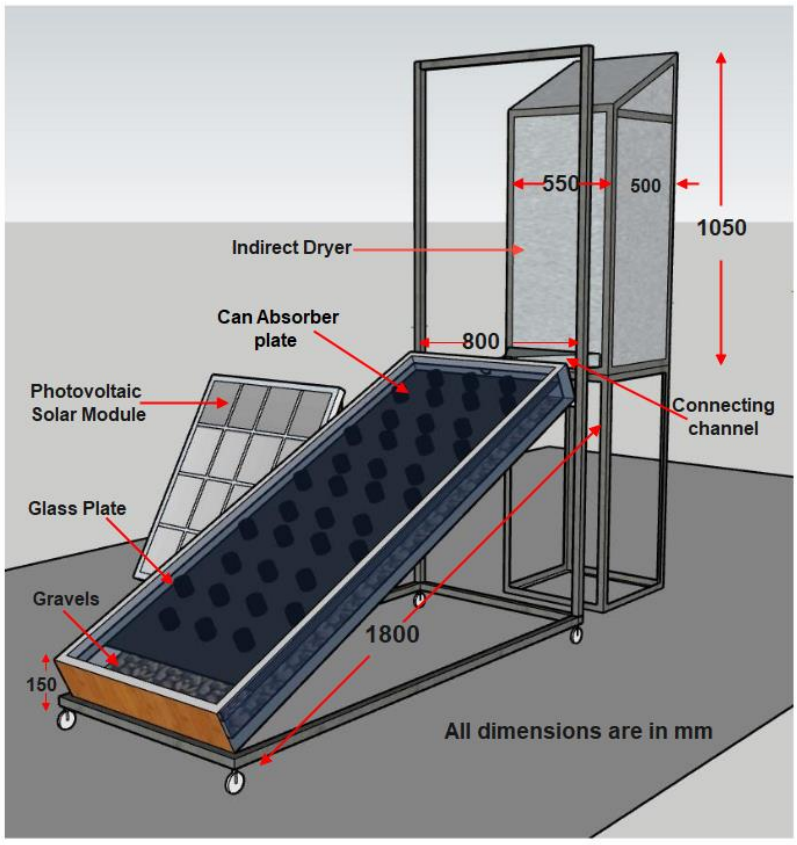

Figure 6.2 Schematic of the experimental setup

Table 6.1 Specification of the drying setup.

Sl No.	Components	Specifications and Materials
1.	Solar Air Collector	
	(i) Area	1.44 m^2
	(ii) Cover Plate	4 mm thick, glass
	(iii) Absorber Plate	1600 mm in length, 800 mm in width, and 1mm in thick aluminium sheet metal incorporated with waste cans
	(iv) Sides of Solar Air Heater	19 mm, Plywood
2.	Sensible Heat Storage	
	Material	gravels (filled up to absorber plate)
3.	Drying Chamber	
	(i) Area	0.27 m^2
	(ii) Chamber Walls	Composite of steel and plywood
	(iii)Maximum capacity of trays	Perforated steel trays, 0.2 m^2 area

6.2 Uncertainty Analysis

Various factors contribute to the lack of precision in measurements, including calibration, environmental conditions, reading errors, and more. The current experiments considered a range of variables such as solar radiation, drying temperature, and the weight of *Curcuma amada*. Eq. (3.1) provides the measurement uncertainty in the result. The maximum uncertainties in $\eta_{e,SAC}$, $\eta_{e,dry}$, $\eta_{Ex,SAC}$ and $\eta_{Ex,dc}$ are 1.35 %, 3.68 %, 2.83 %, and 2.66 %, respectively.

Table 6.2 Uncertainties associated with different parameters in the experiment.

Sl. No.	Instrument	Measured variables	Range	Uncertainty
1	Pyranometer (Amprobe SOLAR-100)	Solar Radiation	0-1999 Wm^{-2}	± 1 (Wm^{-2})
2	Data acquisition system (Libratherm) with thermocouple (PT:100)	Temperature	0 to 200 °C	± 0.1 (°C)
3	Mass balance (A&D Company Limited, (HT-120)	Weight Loss	0-1000 g	± 0.01 (g)
4	Anemometer with RH count Probe (HTC AVM-06)	Velocity	0-30 ms^{-1}	± 0.01 (ms^{-1})

6.3 Thermo-hydraulic performance parameter

To analyse the hydrothermal performance of the canned SAC compared to a flat-plate SAC, thermo-hydraulic performance parameter ($THPP$) is defined. The $THPP$ accounts for the relative gain in Nusselt number in a canned absorber to the pressure drop (pumping power expenditure) due to the presence of obstacles over flat plate collector. If this ratio is greater than unity, then there is a potential benefit of using canned absorber over flat plate collector. The $THPP$ can be expressed as Eq.(6.1) [155]:

$$THPP = \frac{Nu_{CSAC}/Nu_{FSAC}}{(f_{CSAC}/f_{FSAC})^{1/3}} \tag{6.1}$$

where Nu_{CSAC} and Nu_{FSAC} represent the Nusselt number for a canned absorber plate and smooth absorber plate, respectively. The Nu_{CSAC} represents the Nusselt number for a can absorber plate and calculated using Eq. (6.2) [156].

$$Nu_{CSAC} = \frac{hD_h}{k} \tag{6.2}$$

where D_h is the hydraulic diameter of the duct, k is the thermal conductivity in $\mathrm{W/mK}$ and h is coefficient of heat transfer given by Eq. (6.3) [157].

$$h = \frac{\dot{H}_{u,SAC}}{A_{abs}(T_{mp} - T_{av})} \tag{6.3}$$

where T_{mp} is the mean plate temperature and T_{av} is the average of inlet and outlet temperature.

f_{CSAC} denotes the friction factor for the can absorber plate given by Eq. (6.4) [158]

$$f_{CSAC} = \frac{(\Delta P/l)D}{2\rho u^2} \tag{6.4}$$

Nu_{FSAC} signifies the Nusselt number for a smooth absorber plate [157], $Nu_{FSAC} = 0.023Re^{0.8}Pr^{0.4}$ [159] and f_{FSAC} indicates the friction factor for the smooth absorber plate given by the modified Blasius equation [158], $f_{FSAC} = 0.0791\ (Re)^{-0.25}$ [160].

6.4 Exergy sustainability indicators

The improvement potential (IP) is given by Eq. (6.5) [153].

$$IP = \left(1 - \eta_{Ex,dc}\right)\dot{E}x_{l,\,dc} \tag{6.5}$$

The waste exergy ratio (WER) is given by Eq. (6.6) [136].

$$WER = \frac{\dot{E}x_{l,\,dc}}{\dot{E}x_{in,dc}} \tag{6.6}$$

The sustainability index (SI) is calculated using Eq. (6.7) [102]

$$SI = \frac{1}{\left(1 - \eta_{Ex,dc}\right)} \tag{6.7}$$

6.5 Quality Analysis

The process of quality analysis involved converting dried slices of *Curcuma amada* into powder using a mixer grinder. The powdered *Curcuma amada* was then thoroughly sieved for 30 minutes using a vertical vibratory sieve shaker. Subsequently, 15 g of the powder was combined with water in a 1:10 (w/v) ratio, and the mixture was filtered through a Whatman filter paper no.1 from Whatman International, Ltd. Finally, the resulting extracts were stored in a refrigerator at (4 ± 1) °C for further investigations. The total polyphenol content (TPC), total flavonoid content (TFC) and color were tested. The determination of the total phenolic content in *Curcuma amada* extracts was conducted using the Folin-Ciocalteu colorimetric technique as in Lakshmi *et al*. [109]. The total flavonoid content was assessed using the aluminum trichloride method, conducted in accordance with the method

outlined by Hossain *et al.* [66] with some modifications. All determinations were conducted in triplicate. The color of any food product serves as both a symbol of its quality and a psychological factor influencing its acceptance for use. Changes in color over a specific time period can signal the expiration of food products. In the case of *Curcuma amada*, color analysis was conducted to assess the color of dried slices in the dryer. Measurements were taken in terms of L^*, a^*, and b^*values using a Hunter lab Colorimeter. The L^* represents the degree of lightness, while a* indicates redness (positive) or greenness (negative), and b^* indicates yellowness (positive) or blueness (negative) [139]. Total color differences (ΔE; Eq. 6.8) are employed to examine alterations in diverse color characteristics.

$$\Delta E = \sqrt{(\Delta L^*)^2 + (\Delta a^*)^2 + (\Delta b^*)^2} \tag{6.8}$$

6.6 Results and Discussion

The study was performed during March, 2023 with an air mass flux of 0.021 kg/s. The results of an average of six days (similar climatic conditions) were used for each experiment in its performance study. The experiment for SDCWOS took two days and SDCWS was completed in a single day. In both cases, the experiment was conducted from 8:30 h in the morning. Figure 6.3 shows the daily changes in solar radiation along with the hourly variation of atmospheric temperature and inlet and outlet temperatures of SAC, during the experiment. The atmospheric temperature ranged between 24.5 ℃ to 30.2 ℃, 23.1 ℃ to 30.1 ℃, and 24.4 ℃ to 31.2 ℃, respectively for Day 1, Day 2 and Day 3. The maximum inlet and outlet temperatures of SAC were 32.8 ℃ and 68.7 ℃, respectively for Day 1 corresponding to the maximum radiation of 852 W/m^2 at 11:30 h. Similarly, for the maximum solar radiation of 856 W/m^2 on Day 2, the corresponding inlet and outlet temperatures were 32.5 ℃ and 69.1 ℃. Both Day 1 and Day 2 were performed without SHS. The use of SHS on Day 3 led to an increase in the outlet temperature of SAC. The inlet and outlet temperatures on Day 3 were 35.9 ℃ and 78.8 ℃ for a solar radiation of 860 W/m^2. The outlet temperature showed a substantial increase in SDCWS than in SDCWOS. The conditions necessary for speeding up drying process are elevated drying air temperatures, flow rate, layer thickness. The observed phenomenon in Figure 6.3, where the outlet temperature of the solar collector with storage is higher than that of the solar collector without storage in the morning, contrary to the typical expectation that the storage material absorbs energy from the absorber, resulting in a lower temperature. Upon careful consideration, it has been observed that this result is influenced by the early sunrise in northeastern states of India. It is important to note that data collection for both the solar

collector and the dryer starts at 8:30 am. However, preheating of solar absorber was done from 7.30 a.m. and within this one hour, both storage material and the canned absorber reached the near steady state temperature. Because of the early sunrises, the swift rise in solar intensity during the early morning hour can significantly impact the temperature dynamics. In this context, the higher outlet temperature in the solar collector with storage has attributed to the system absorbing and utilizing solar energy at an earlier stage in the day coupled with enhanced heat transfer to the air by reducing plate mean temperature once experiment started. Therefore, the observed temperature pattern has been associated to geographic and temporal factors, specifically the early sunrise, influencing the temperature readings during the data collection period. Figure 6.4. illustrates the changes in the dryer inlet and outlet temperatures. The inlet temperature varied in the range of 41.8 ℃ to 61.2 ℃ for SDCWOS and 45.6 ℃ to 62.1 ℃ for SDCWS. The dryer inlet temperature is lower than the SAC outlet temperature in both cases, due to some energy loss via convection in the connecting passage. For SDCWOS, the dryer outlet temperature varied between 37.1 ℃ and 52.4 ℃, while for SDCWS, it ranged from 40.2 ℃ to 51.1 ℃. Overall drying times were 26 and 10 h for SDCWOS and SDCWS, respectively. SDCWOS required over a day to reach the final MC of 4.4 % (w.b.) from 87.1 % (w.b.), extended until 10:30 h on the second day. In contrast, SDCWS completed the experiment within a day to achieve the final MC. Subsequently, with reduced solar radiation and lower surrounding temperatures, both collector and dryer temperatures decreased.

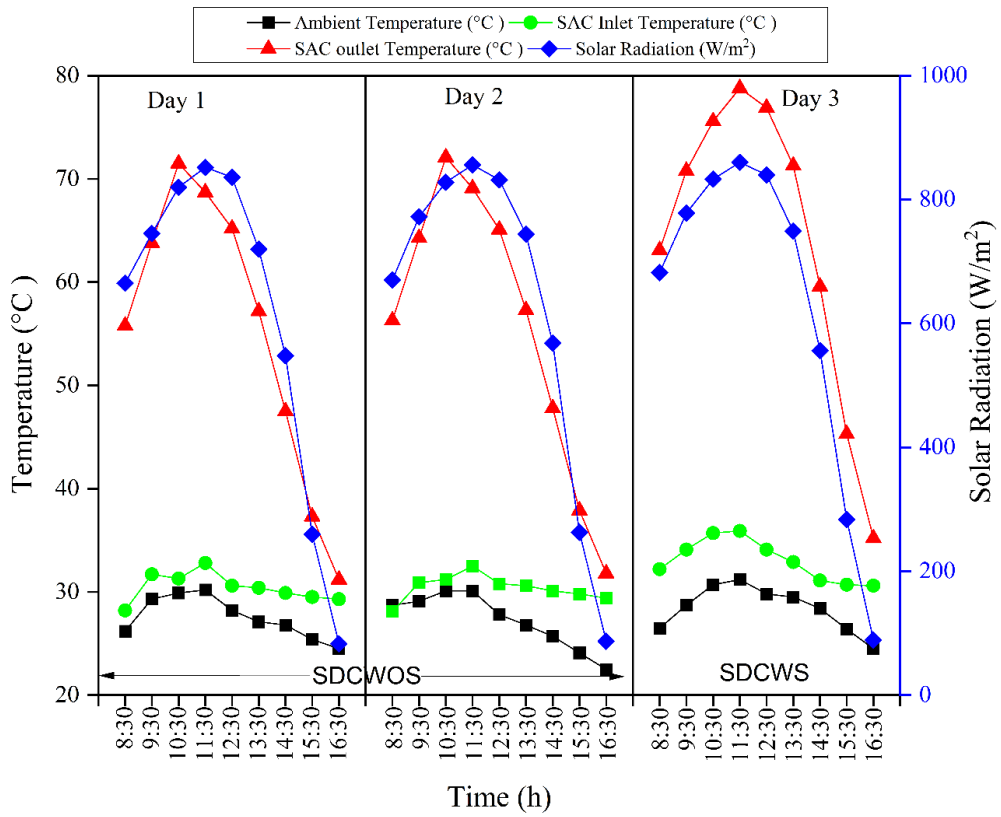

Figure 6.3 Changes in Temperature and Solar Radiation over time in SDCWOS and SDCWS.

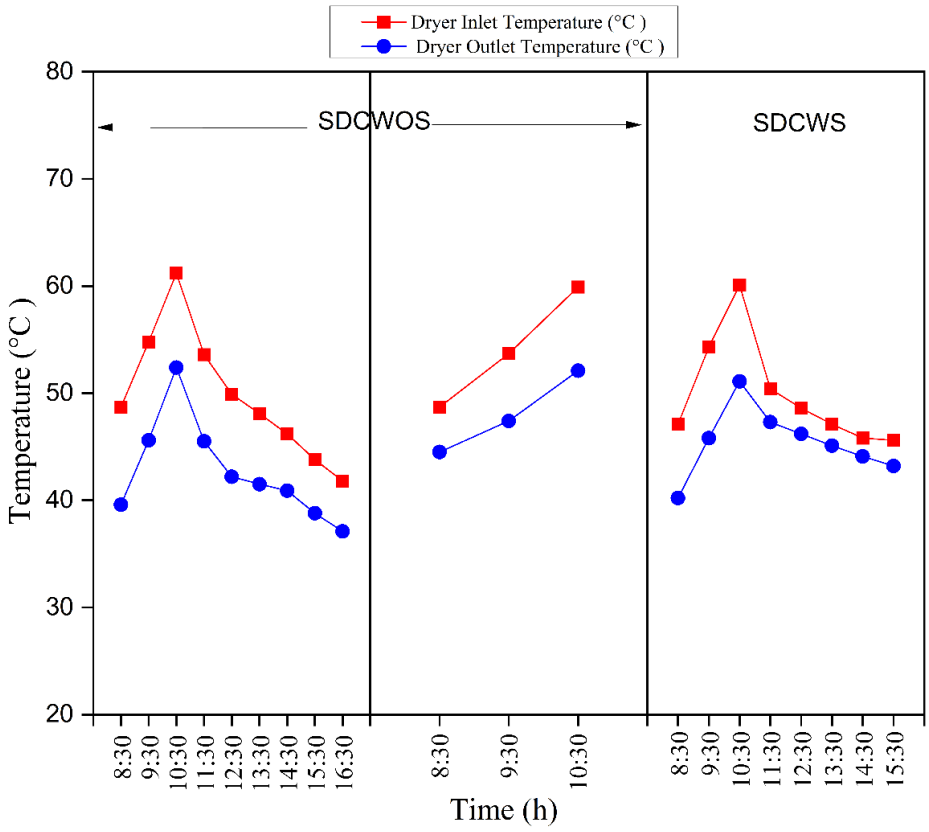

Figure 6.4 Changes in dryer inlet temperature and dryer outlet temperature with drying time

6.6.1 Drying Kinetics

The two mentioned conditions were used as the basis for conducting drying tests. The initial MC of the *Curcuma amada*, was determined to be 87.1 % (w.b.) using the hot-oven method. Figure 6.5 illustrates the variation of MC over time for SDCWOS and SDCWS. The ultimate MC dropped to 4.4 % (w.b.) within a span of 26 h for SDCWOS, while achieving the same reduction for SDCWS took only 8 h. To ensure uniform drying, the trays loaded with *Curcuma amada* were exchanged at regular intervals throughout the experiment. The results showed that the moisture removal from the surface occurred more rapidly during the early stages of drying. Moreover, the drying temperatures achieved in SDCWS were higher than in the SDCWOS, as expected, resulting in shorter drying times.

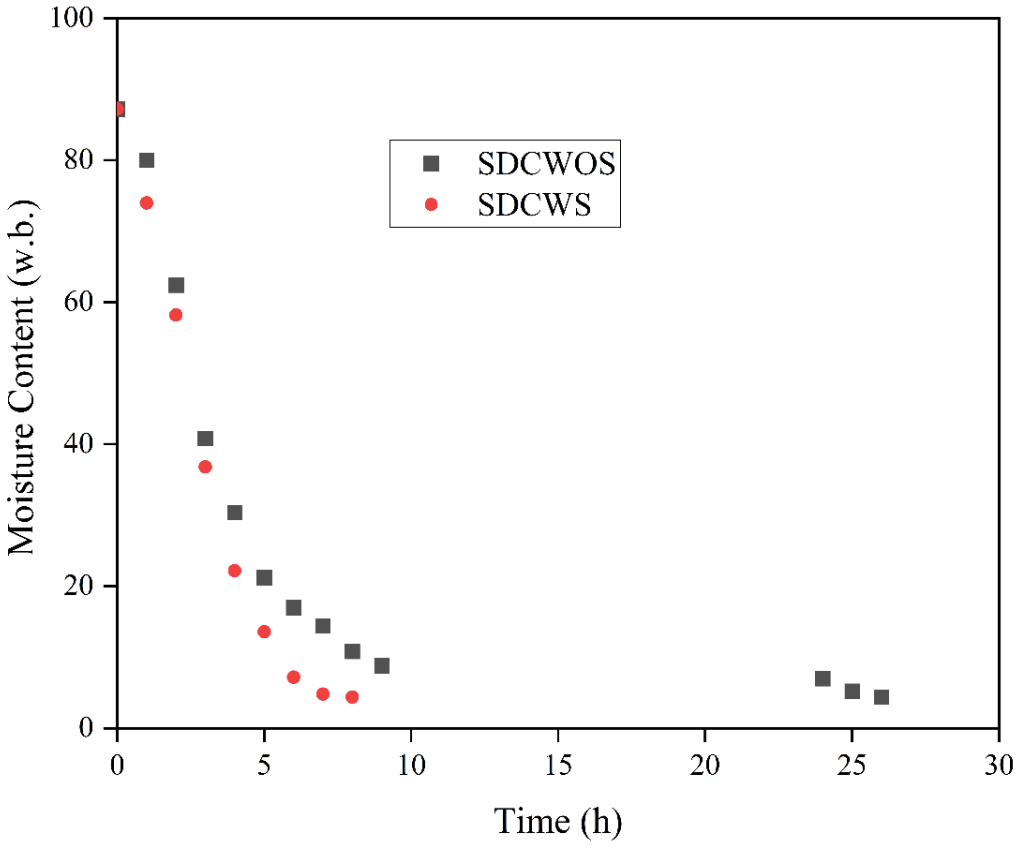

Figure 6.5 Variations of MC with time

The study involved the assessment of eleven models from existing literature to identify suitable drying models for two sets of experiments conducted in a solar dryer. Figure 6.6 illustrates the changes in MR concerning drying time for SDCWOS and SDCWS. To determine the most appropriate fitting of drying model from the eleven options in Table 3.2,

a non-linear regression analysis of MR against drying time was essential. Tables 6.3 and 6.4 provide a summary of the regression analysis results for SDCWOS and SDCWS, respectively. The evaluation involved assessing all eleven models based on the criteria of achieving the highest R^2 value and the lowest values of χ^2, and $RMSE$. After meeting these conditions, the Midilli and Kucuk model emerged as the best-fit model for *Curcuma amada* in both SDCWOS and SDCWS. The respective values were $R^2 = 0.9973$, $\chi^2 = 0.00010$, and $RMSE = 0.01839$ for SDCWOS and $R^2 = 0.999$, $\chi^2 = 0.00009$, and $RMSE = 0.01364$ for SDCWS.

The Midilli and Kucuk model for SDCWOS is given as:

$$MR = 1.531\, exp(-0.4286t^{0.8654}) + 0.002541\, t \tag{6.10}$$

The Midilli and Kucuk model for SDCWS is given as:

$$MR = 1.027\, exp(-0.1056t^{1.857}) + 0.006113\, t \tag{6.11}$$

Figure 6.7 and Figure 6.8 show the comparison of experimental and predicted MR for SDCWOS and SDCWS using the Midilli and Kucuk model. The straight line for SDCWOS and SDCWS validates the model's suitability, as this may be seen in these figures.

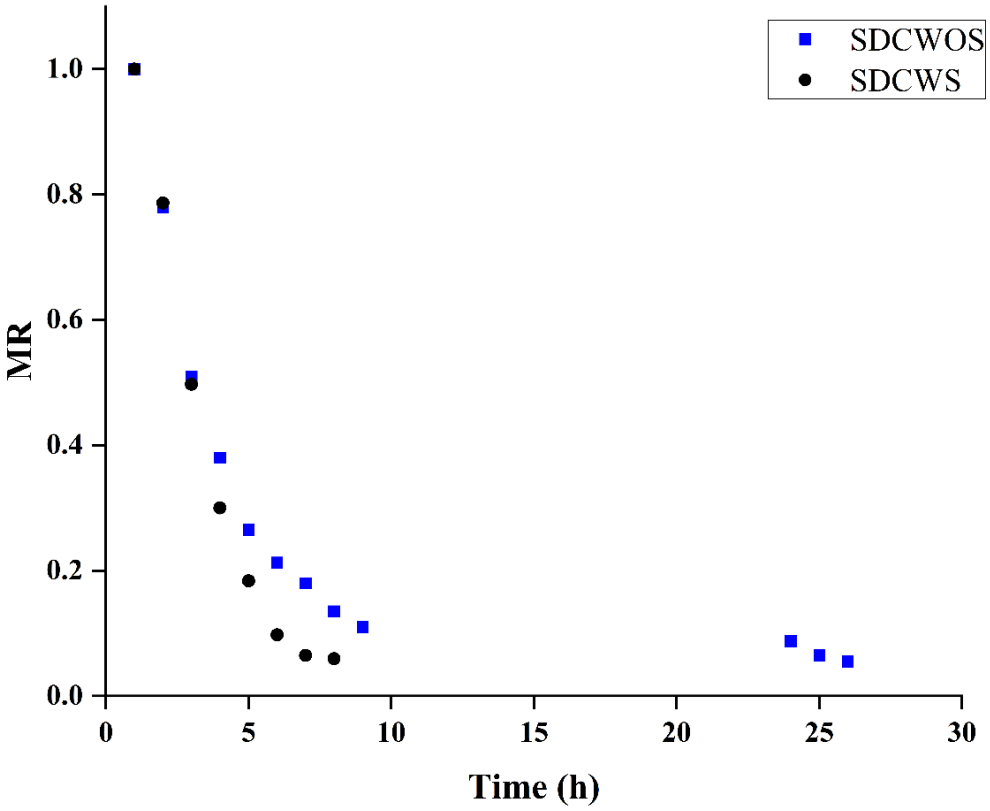

Figure 6.6 Variations of MR with time

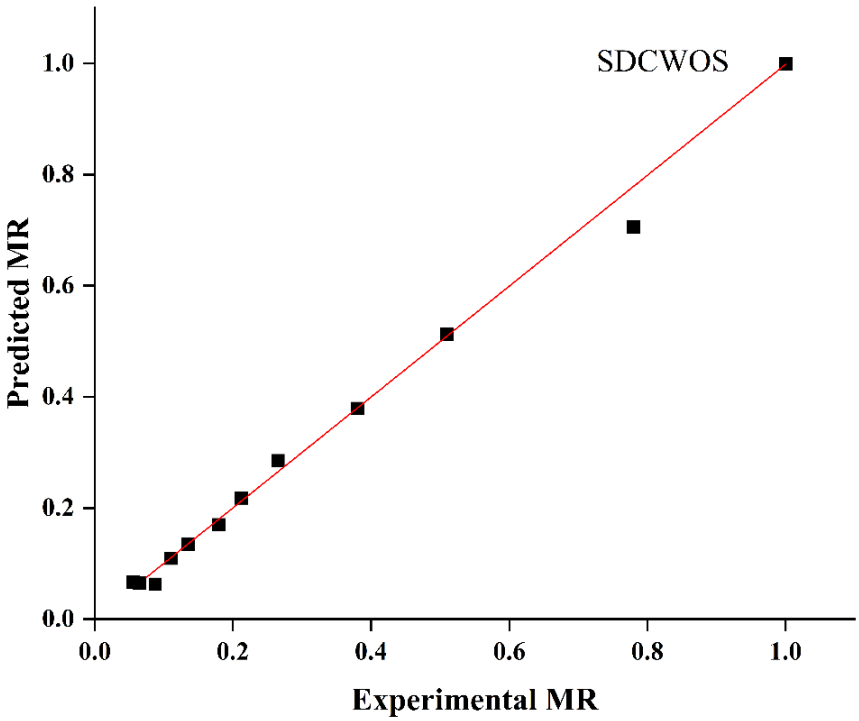

Figure 6.7 Comparison of predicted and experimental MR for SDCWOS

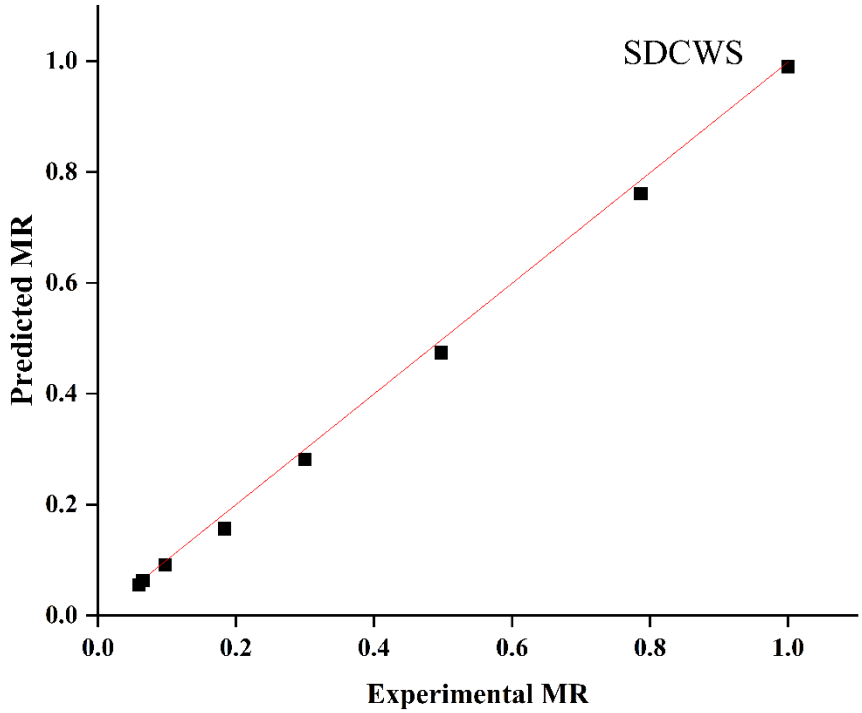

Figure 6.8 Comparison of predicted and experimental MR for SDCWS

Table 6.3 Fitting statistics of thin layer drying model of SDCWOS.

Model No.	Coefficients and constants	R^2	χ^2	$RMSE$
A.	$k = 0.2227$	0.9185	0.00318	0.08672
B.	$k = 0.1115;\ n = 1.471$	0.9595	0.00158	0.06411
C.	$k = 1.3; n = 0.1713$	0.9185	0.00318	0.09095
D.	$k = 1.371; a = 0.3095$	0.9803	0.00077	0.04473
E.	$a = 0.7815; b = -0.1499;\ c = 0.8508;$ $g = 0.2135; h = 0.2152;\ k = 0.5294$	0.9818	0.00071	0.05546
F.	$a = 1.385; k = 0.06503; c = 0.368$	0.9955	0.00018	0.022
G.	$a = -26.76;\ k_1 = 28.05;\ b = 0.2797;\ k_2 = 0.2802$	0.9782	0.00085	0.05259

H.	$a = 2.165;\ k = 0.3961$	0.9723	0.00108	0.05301
I.	$a = -0.149;\ b = 0.004461$	0.9213	0.00307	0.08937
J.	$a = 0.9997;\ b = -0.9378;\ k = 0.2242$	0.9296	0.00275	0.0891
K.	$\boldsymbol{a = 1.531;\ b = 0.002541;}$ $\boldsymbol{k = 0.4286;\ n = 0.8654}$	**0.9973**	**0.00010**	**0.01839**

Table 6.4 Fitting statistics of thin layer drying model of SDCWS.

Model No.	Coefficients and constants	R^2	χ^2	$RMSE$
A.	$k = 0.2841$	0.8944	0.01005	0.1072
B.	$k = 0.1018;\ n = 1.785$	0.9944	0.00053	0.02656
C.	$k = 1.197; n = 0.2373$	0.8944	0.01005	0.1158
D.	$k = 1.452; a = 0.4019$	0.9843	0.00150	0.04464
E.	$a = 0.2445; b = 1.21;\ c = -0.09846;$ $g = 0.4022; h = 8.634;\ k = 0.4047$	0.9843	0.00150	0.07732
F.	$a = 1.449; k = -0.08363; c = 0.3307$	0.9892	0.00103	0.04051
G.	$a = -0.1629;\ k_1 = 1.613;$ $b = 0.4181;\ k_2 = 0.4032$	0.9843	0.00149	0.05466
H.	$a = 2.231;\ k = 0.4987$	0.9961	0.00037	0.02222
I.	$a = -0.2104;\ b = 0.01084$	0.9536	0.00442	0.07674
J.	$a = 7.205;\ b = 0.8058;\ k = 0.09834$	0.9452	0.00522	0.09138
K.	$\boldsymbol{a = 1.027;\ b = 0.006113;}$ $\boldsymbol{k = 0.1056;\ n = 1.857}$	**0.999**	0.00009	**0.01364**

6.6.2 Energy Analysis

The changes in thermal efficiencies of the SAC are plotted in Figure 6.9. The performance of SAC, as defined by Eq. (3.9), is impacted by various factors such as rate of mass flow, the area of SAC, temperatures of inlet and outlet and the amount of solar radiation it receives. The average thermal efficiencies were 66.79 %, 67.74 %, and 87.95 %, respectively, for Day 1, Day 2 (SDCWOS) and Day 3 (SDCWS). The collector with gravels demonstrated higher average efficiencies in contrast to those without storage. This difference in efficiency may be attributed to the energy storage material, which absorbs excess heat during the day and releases it during low solar radiation. As a result, the system can provide hot air into the late hours, leading to an increased efficiency. The study by Abdelkader *et al.* [161] and Kalaiarasi *et al.* [162] showed similar trends for the efficiency of the collector with storage.

The energy efficiency and SEC of the dryer, both with and without storage, is illustrated in Figure 6.10 and calculated using Eq. (3.11) and (3.12), respectively. The efficiency in every instance was contingent upon the extraction of MC from *Curcuma amada*. The mean dryer efficiency for SDCWOS was 21.88 %, while for SDCWS, it stood at 29.63 %. The average SEC was 17.26 kWh/kg and 11.29 kWh/kg, for SDCWOS and SDCWS, respectively. In similarity, a solar dryer was developed using indirect and mixed-mode approaches without storage for tomato drying [34]. The drying durations were 26 h for indirect mode and 17 h for mixed mode, yielding efficiencies of 8.80 % and 10.66 %, respectively. Vijayan *et al.* [84] applied a mathematical model to explain the operation of an active solar collector employing SHS (pebble) material for drying bitter gourd, resulting in a drying time of 7 h and an efficiency of 19 %. In another distinct examination, Ayyappan *et al.* [47] conducted a comparison of various SHS materials, including concrete, sand, and rock bed, to assess their thermal performance. The drying times for Copra in a greenhouse dryer utilizing concrete, sand, and rock bed were 78 h, 66 h, and 53 h, respectively, with corresponding efficiencies of 9.5 %, 11 %, and 11.65 %. SDCWOS took two days to dry the product whereas the product was dried in a single day in SDCWS. On the second day, as the moisture level of the drying material decreased within the SDCWOS system, a lesser amount of energy was utilized to remove the remaining moisture. This led to reduced utilization of heat energy in the dryer, causing a drop in its thermal efficiency and an increase in SEC. However, in both cases the SEC increased towards the end due to lesser removal of MC. When comparing the two, the dryer integrated with gravels demonstrated superior efficiency

in comparison to the dryer without storage. This can be primarily attributed to the fact that the average outlet temperature of the SAC with storage was higher than that of the collector without storage. Consequently, this elevated the inlet temperature of the solar dryer, leading to a more efficient removal of moisture in a shorter timeframe.

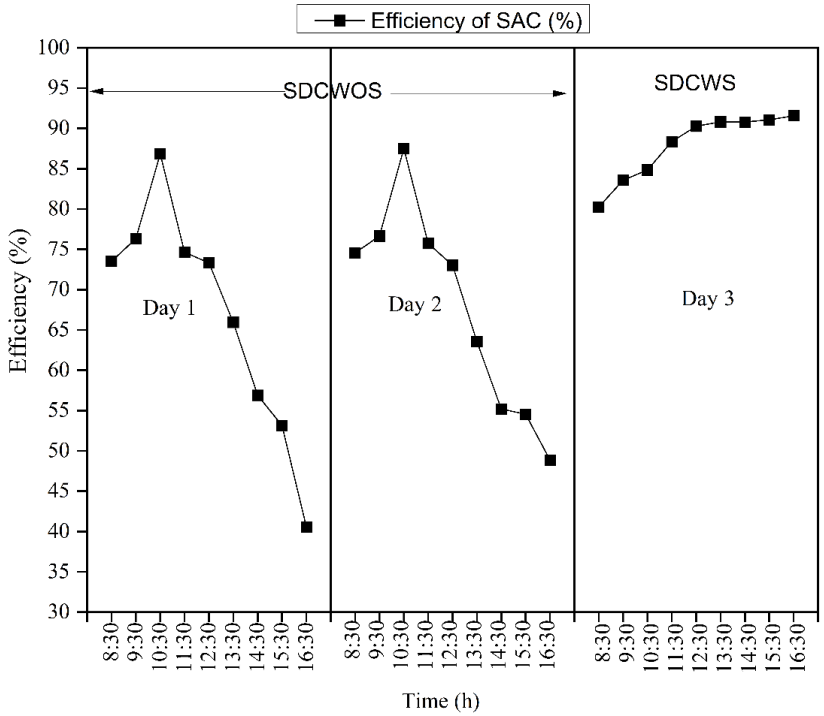

Figure 6.9 Changes in efficiency of canned solar air collector with time

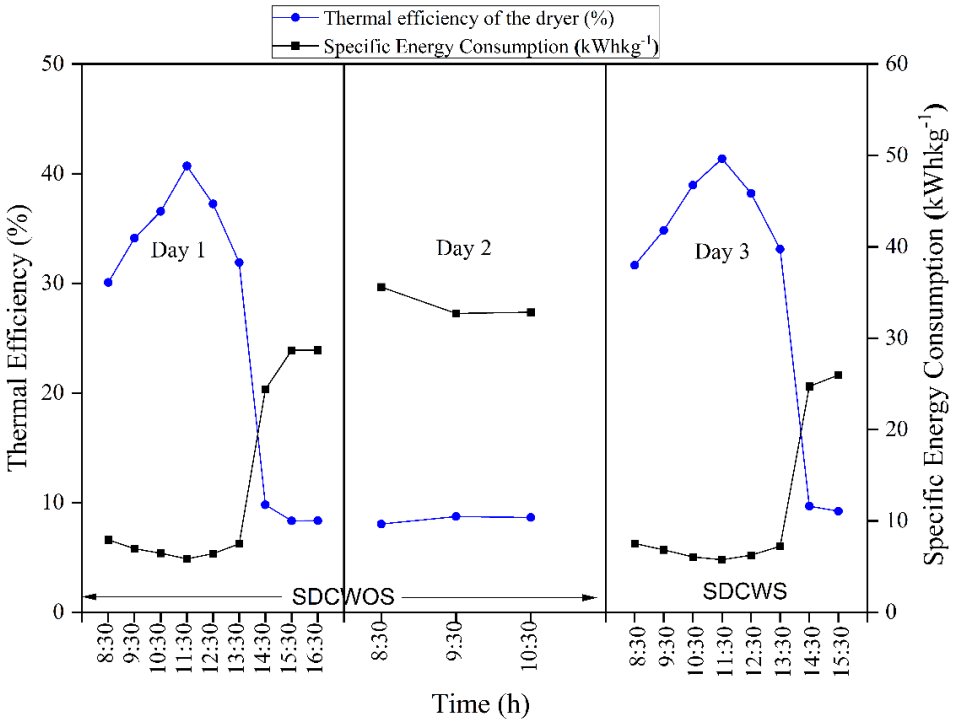

Figure 6.10 Changes of efficiency and SEC in SDCWOS and SDCWS with drying time

The effect of solar radiation on the performance of the dryer may be examined from the Figure 6.11. The efficiency of the dryer, both SDCWOS and SDCWS, increases with the increase of solar radiation. It can be observed that the efficiency of the solar dryer is directly depended on the solar radiation particularly during the initial four hours of drying.

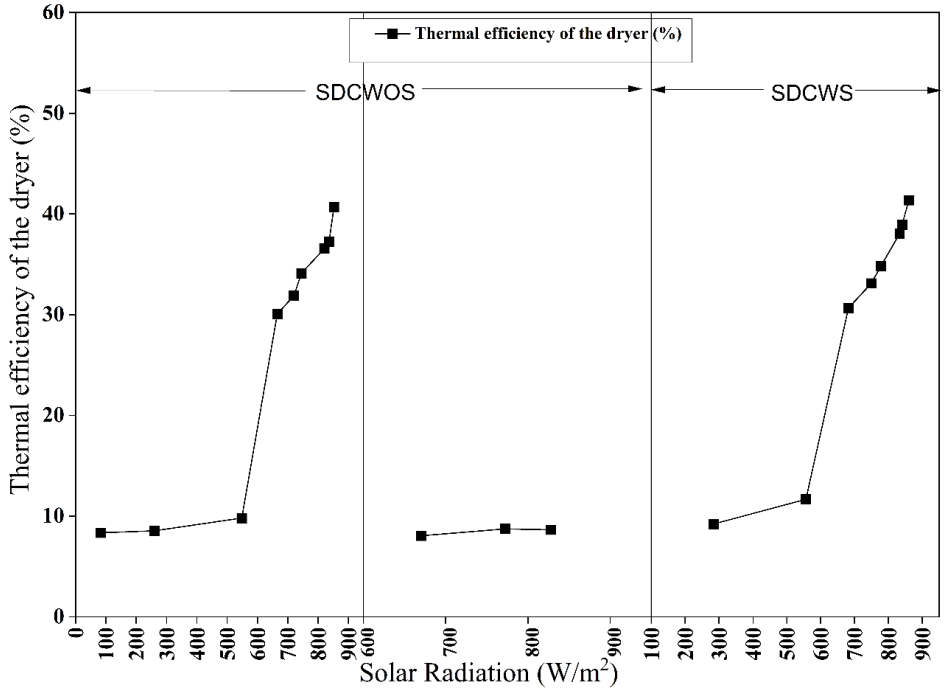

Figure 6.11 Variation of efficiency with solar radiation

The Figure 6.12 illustrates the thermo-hydraulic performance parameter ($THPP$) for the canned SAC with and without storage. The $THPP$ showed above 1.0 for both SDCWOS and SDCWS for four hours of experimentation at constant air mass flow rate. This suggests that the enhancement in Nusselt number relative to the increase in friction is comparatively higher when cans are integrated in flat absorber. The results are in close agreement with the observations reported by Madadi *et al.* [155] which showed that the absorber plate with vertical cylinder showed average $THPP$ of 1.2. Singh Patel and Lanjewar [163] in another study of V-rib geometry SAC calculated the highest $THPP$ of 1.59.

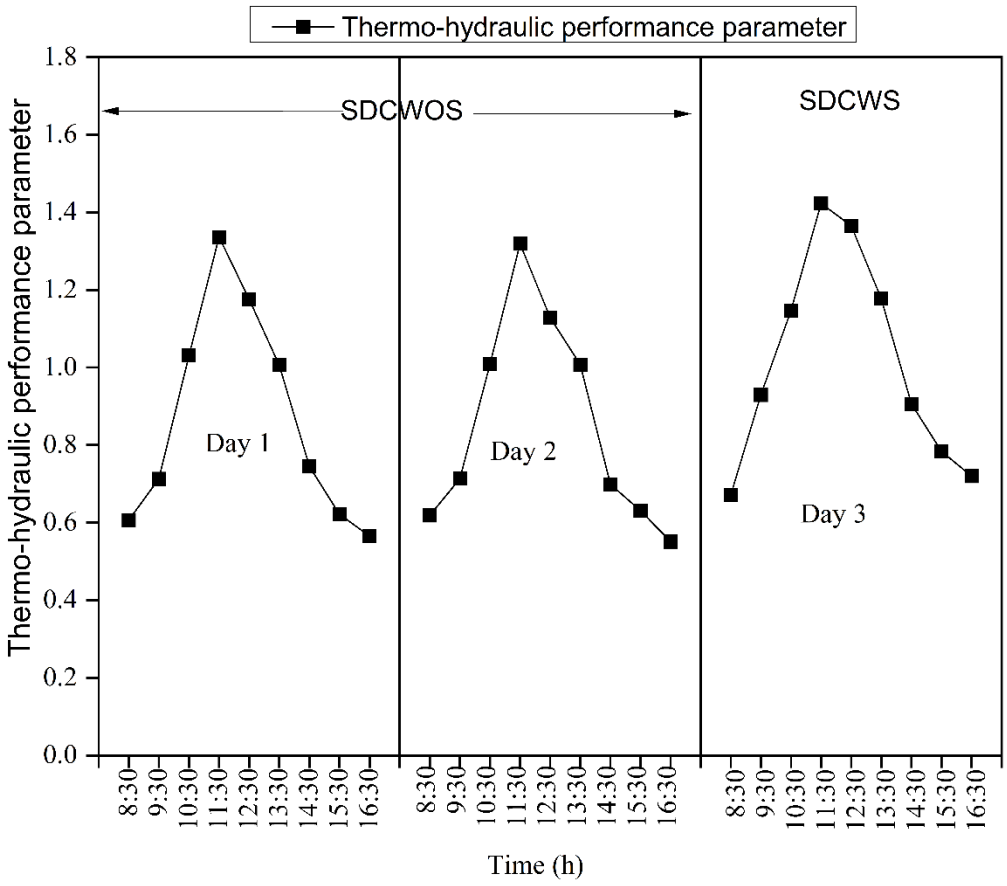

Figure 6.12 Variation of thermo-hydraulic performance parameter with time

6.6.3 Exergy Analysis

The exergy study is valuable for identifying potential improvements and reducing losses to enhance system effectiveness [164]. To evaluate the effectiveness of SAC, exergy input, exergy output, exergy loss, and exergy efficiency were computed using Eqs. (5.5), (5.7), (5.8) and (5.9), respectively. Figure 6.13 displays the variation of exergy in, out, and loss in the dryer. The exergy in in SAC ranged from 96.11 W to 985.71 W, 100.78 W to 990.36 W, and 103.06 W to 994.81 W, respectively for Day 1, Day 2, and Day 3. The exergy out varied from 7.42 W to 319.28 W, 13.06 W to 323.13 W, and 24.07 W to 382.43 W, respectively for Day 1, Day 2, and Day 3. The lowest values were observed at 16:30 h for the days lacking storage, aligning with solar radiation levels ranging from 83 to 87 W. Similarly, for the days featuring storage, the minimum values also occurred at 16:30 h, coinciding with solar radiation of 89 W. The SAC with storage helped the absorber plate to maintain higher temperatures even after solar radiation decreased. This resulted in reduced exergy loss. The exergy loss ranged from 88.69 W to 706.14 W, 87.71 W to 704.14 W, and 78.98 W to 616.25 W for Day 1, Day 2, and Day 3, respectively. Exergy losses are more

significant at noon due to the higher solar radiation, temperature and it was observed within the h of maximum sunlight [165]. The exergy in, out, and loss followed similar patterns with solar radiation [112]. The mean exergy efficiency was computed as 22.78 %, 23.52 %, and 33.68 % for Day 1, Day 2, and Day 3, respectively.

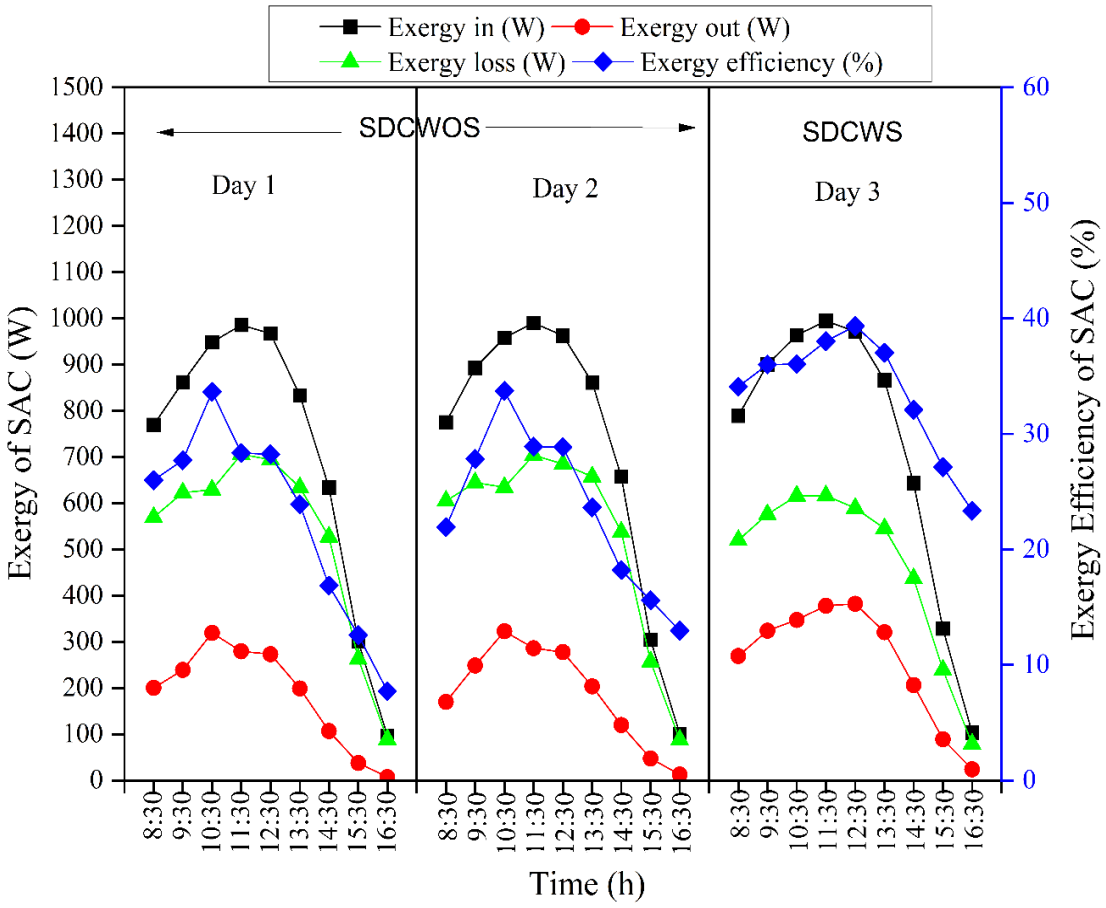

Figure 6.13 Changes of exergy in, out, loss, and efficiency of canned solar air collector with drying time

An exergy study serves as a valuable tool for enhancing the efficiency of solar drying processes, determining the energy requirements for drying, and identifying the type of energy needed [166]. It also allows for examining the direction of irreversible processes and their consequences. The exergy in, out, loss, and efficiency of the drying cabinet are determined using Eqs (5.10), (5.11), (5.12), and (5.13), respectively. Figure 6.14 illustrates the changes in exergy input, exergy output, exergy loss, and exergy efficiency concerning drying time for both SDCWOS and SDCWS. The results reveal that solar radiation significantly impacts the exergy inflow, outflow, and losses, causing a rise in the temperature within the dryer. The distinction between the exergy input and output of the solar dryer is

referred to as exergy loss. The graphs demonstrate that during the early h of the day (up to 10:30 h), there is a rise in exergy input, exergy output, and exergy loss, followed by a decline during the latter portion of the day for all the two scenarios. The average exergy inflow was calculated as 128.2 W and 111.05 W for SDCWOS and SDCWS, respectively. Meanwhile, the average exergy outflows were 69.84 W and 72.89 W, respectively. The exergy efficiencies ranged from 41.18 % to 66.59 %, and 49.57 % to 83.65 % for SDCWOS and SDCWS, respectively. As the drying process progresses through the hour of the day, the exergy efficiency experiences a gradual enhancement. This increase in exergy efficiency stems from the exergy output approaching the exergy input of the drying cabinet. Moreover, the final stage of dehydration records the highest exergy efficiency. This occurs because as the dehydration process nears completion, there is less moisture left in the product, resulting in lower energy consumption during the last stage of drying. The findings closely align with those reported by Bareen *et al.* [167]. They developed an indirect-type forced convection solar dryer incorporating phase change material (PCM) for energy storage, specifically for the drying of Cymbopogon citratus. The exergy efficiency of the drying chamber ranged from 47 % to 97 %. Further, Silva *et al.* [97] found the exergy efficiency to be 10 % and 66 % in a solar dryer for drying corn grains. Comparable findings were documented in the assessment of energy and exergy aspects during the drying of olive mill wastewater (OMW) employing an indirect natural convection solar dryer [168]. Throughout the two-day experimental procedure, the exergetic efficiencies of the drying chamber ranged between 34.4 % and 100 %.

A sustainable drying section can be created by employing the exergetic sustainability indicators like IP, WER and SI. These indicators were calculated to assess the exergy efficiency and losses in the drying section relative to the exergy input and is presented in Table 6.5. The mean IP values for the two cases were 20.71 and 15.23 W, respectively. The configuration without storage exhibited a higher IP compared to the one with storage, indicating minimal exergy loss. The value of WER lies between 0 and 1. A value near zero signifies a more efficiently sustainable system (as in SDCWS), as it effectively harnesses useful exergy. Conversely, a value approaching one (as in SDCWOS) indicates a system that is not very efficient [153]. The SI is elevated in the configuration with storage, signifying greater exergy efficiency compared to the configuration without storage.

Table 6.5 Summary of *IP*, *WER* and *SI* for SDCWOS and SDCWS.

Property	SDCWOS		SDCWS	
	Range	Average	Range	Average
IP (W)	11.09-44.58	20.71	2.10-36.85	15.23
WER	0.33-0.58	0.37	0.16-0.50	0.31
SI	1.70-2.99	2.68	1.98-4.90	3.90

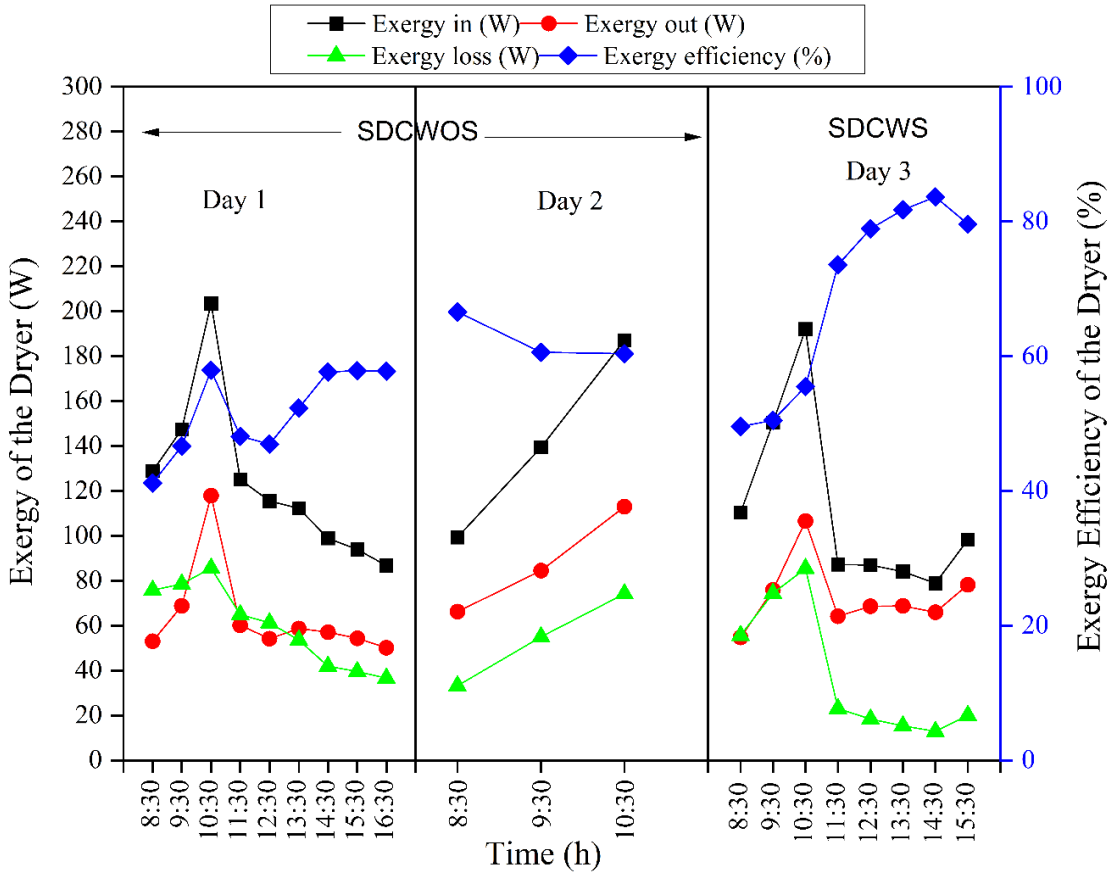

Figure 6.14 Changes of exergy in, out, loss, and efficiency in SDCWOS and SDCWS with drying time

6.6.4 Mass shrinkage ratio

The calculated mass shrinkage ratio (*SR*) of the dried *Curcuma amada* is determined from Eq. (5.14). SR of SDCWOS and SDCWS for the first day of drying is given in Figure 6.15. In the beginning, with a high MC in the *Curcuma amada*, the exergy efficiency is typically low because a significant amount of energy is required to remove moisture. As time progresses, the rate of shrinkage diminishes as the MC decreases, leading to an increase in exergy efficiency. This happens because less energy is required to remove moisture from the near drying material. This showed significant shrinkage of *Curcuma amada* in SDCWS compared to SDCWOS.

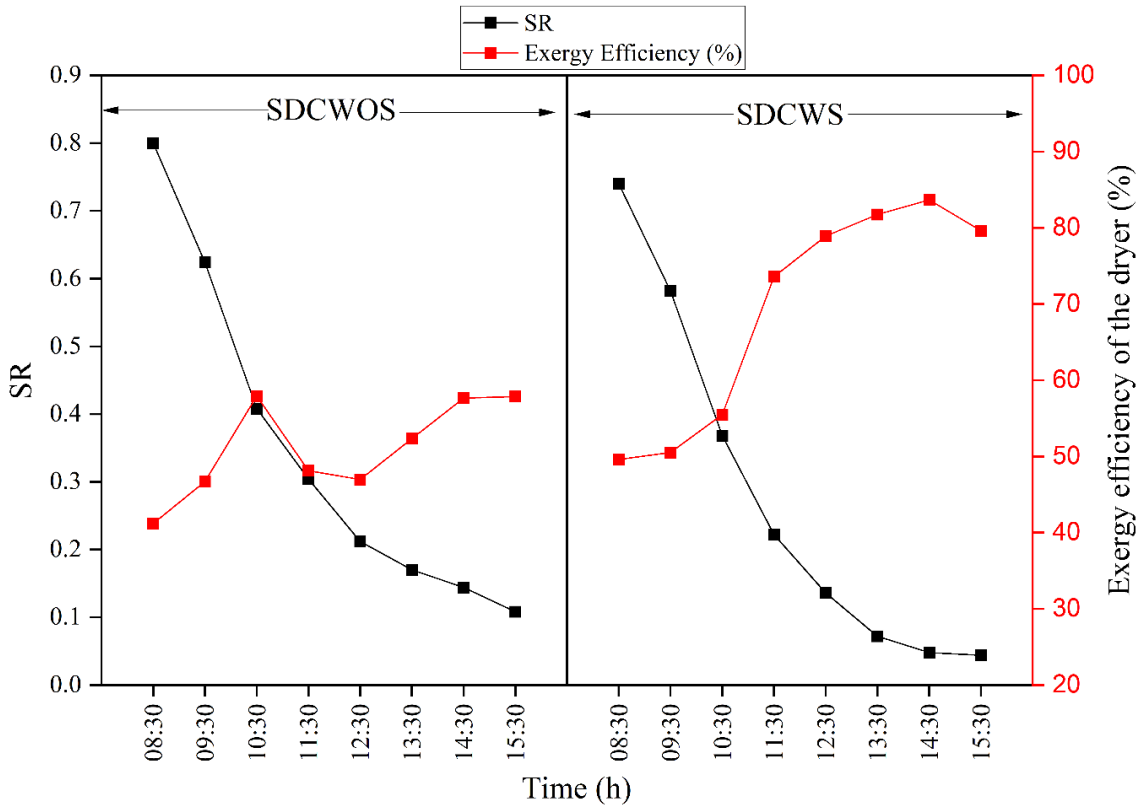

Figure 6.15 Variations of SR and Exergy efficiency of the dryer with time for SDCWOS and SDCWS

6.6.5 Quality Analysis

The TPC of the dried *Curcuma amada* were determined using Folin-Ciocalteu's reagent. The TPC was measured to be 39.01 mg/100g for SDCWOS and 46.02 mg/100g for SDCWS. The TPC of fresh juice of *Curcuma amada* as reported by Policegoudra and Aradhya [169] was measured as 20.8 mg/100 g for temperatures 25 ℃ and 14 ℃. The rise in TPC in the current study has increased due to the release of phenolic contents from the

matrix during the drying processes. Phenolic contents, naturally bound, break down cell constituents and are rapidly released during drying methods [142]. The total flavonoid content was further observed in dried *Curcuma amada*. The TFC was measured as 25.02 mg/100 g and 33.04 mg/100 g for SDCWOS and SDCWS, respectively. The longer duration of drying attributed to the decrease of TFC. Colour represents one of the most crucial sensory attributes of a food product. In this investigation, the colour of the dried samples was assessed using a Hunter Lab colorimeter. Before drying, the average L^* value for the fresh *Curcuma amada* treatment was 64.26. However, after drying, substantial changes in values were observed, ranging from 81.97 (SDCWOS) to 74.55 (SDCWS), when using the developed dryer. The a^* was 0.70, 2.89, and 3.75 for fresh, SDCWOS and SDCWS, respectively. The rise in a^* values could be linked to the reduction in camphor content [139]. The yellowness of *Curcuma amada* remained same in SDCWOS (19.50), SDCWS (20.48) and fresh sample (21.41) as indicated by b^* parameter. Mean surface colour values of dried *Curcuma amada* under solar drying are evaluated using Eq. (6.8). The value of ΔE is 17.94 and 10.77 for SDCWOS and SDCWS, respectively. The value ΔE , of the sample dried in SDCWOS is noted to be greater than that of the sample dried using SDCWS.

6.6.6 Economic Analysis

The economic growth of a product is heavily reliant on its processing method. Currently, the costs of the solar dryers were 22,000 INR and 23,000 INR for SDCWOS and SDCWS, respectively. For both cases, the price includes the cost of SAC. The rate of inflation has been set at 7.79 %, while the interest rate is 10 %. 20 years is considered as the projected longevity of the dryer. To evaluate the economic advantages of the developed dryer over the long term, an analysis of life cycle savings has been conducted, alongside the determination of the payback period, a crucial measure of its economic viability. Table 6.6 provides the estimated prices of SDCWOS and SDCWS, respectively. The cost savings achieved by employing solar energy for drying *Curcuma amada* have been computed by contrasting it with commercially available *Curcuma amada* sold in the market. In the Indian market, *Curcuma amada* is marketed for 890 INR per kg. The first-year savings have been calculated as 14282 INR and 52598 INR for SDCWOS and SDCWS, respectively, considering 150 days per year. The payback period is estimated as 1.7 years and 0.47 year for SDCWOS and SDCWS, respectively. The payback period is significantly lower than the useful life of 20 years of the dryer. However, given the diverse drying of seasonal vegetables and fruits all year round, the expected payback period is predicted to further decrease,

rendering it considerably short in comparison to the lifespan of the dryer. The results of the present investigation align with those of Sethi *et al.* [112], whose study suggested that the payback period of the dryer 0.48 year for drying of potato chips. Another study was conducted to model the performance of a cocoa bean dryer under different convection scenarios: natural, forced, and a combination of forced and natural convection [130]. The aim was to assess their efficiency in a tropical climate. The analysis revealed a calculated payback period of 2.19 years.

Table 6.6 Estimated prices of SDCWOS and SDCWS

Particulars	SDCWOS	SDCWS
Cost of the dryer with integrated SAC in INR	22000	23000
Projected duration of the life of the dryer in years.	20	20
Cost of fresh *Curcuma amada* in INR	75	75
Rate of interest	10 %	10 %
Rate of inflation	7.79 %	7.79 %
Yearly capital cost in INR	2584	2702
Cost of maintenance in INR	258	270
Salvage value in INR	2200	2300
Yearly salvage value in INR	38	40
Yearly cost in INR	2804	2932
Cost of dry *Curcuma amada* in INR	890	890
Savings in INR	95	351
Yearly savings in INR for the first year	14282	52598
Payback period in years	1.7	0.47
(1 US$=74.57 INR)		

In Chapter 3 of the study, it was estimated that the dryer had a lifespan of 10 years, whereas in this chapter, the lifespan was extended to 20 years. The change in these estimations is considered due to the structural differences between the systems analysed in the respective chapters. Specifically, Chapter 3 focuses on a direct dryer while this chapter examines an indirect dryer featuring a canned absorber plate. The choice of the dryer plays a pivotal role in determining the durability and longevity of the dryer. The direct dryer utilized in Chapter 3 presents certain limitations in comparison to the indirect solar dryer

employed in this chapter. The dryer in this chapter was innovative with waste cans integrated with the SAC that increased the thermal performance. Moreover, even with a lifespan of 10 years, the new design in the current chapter will offer more return on investment compared with the previous design mentioned in Chapter 3.

6.7 Comparisons of the different modes of solar dryer in terms of performance

Table 6.7 gives the comparisons of the different modes of solar dryer developed in the current study in terms of performance. The findings indicate that, among the studied dryers, mixed-mode solar drying with corrugated absorber plate SAC with SHS for *Garcinia pedunculata* and indirect solar drying integrated with canned absorber plate SAC with SHS for *Curcuma amada*, demonstrated superior performance.

Table 6.7 Comparison of different modes of solar dryer.

Sl No	Type of dryer	Product	Drying Time (h)	Drying Kinetics	Thermal efficiency (%)	Payback period (year)
1	Free convection corrugated type	*Garcinia pedunculata*	28	Midilli and Kucuk	10.77	0.6
2	Indirect solar drying with corrugated absorber plate SAC but without SHS	*Garcinia pedunculata*	31	Two-Term model	18.12	1.6
3	Mixed-mode solar drying with corrugated absorber plate SAC but without SHS	*Garcinia pedunculata*	26	Two-Term model	22.37	0.9
4	Indirect solar drying with corrugated absorber plate SAC with SHS	*Garcinia pedunculata*	28	Two-Term model	21.74	1.4

5	Mixed-mode solar drying with corrugated absorber plate SAC with SHS	*Garcinia pedunculata*	10	Midilli and Kucuk	24.46	0.59
6	Indirect solar drying integrated with canned absorber plate SAC but without SHS	*Curcuma amada*	26	Midilli and Kucuk	21.88	1.7
7	Indirect solar drying integrated with canned absorber plate SAC with SHS	*Curcuma amada*	8	Midilli and Kucuk	29.63	0.47

6.8 Summary

This set of experiments were performed to check the variability and practical implication of the solar dryer. Therefore, the indirect solar dryer mode for drying of *Curcuma amada* was combined with a solar air collector (SAC) featuring an absorber plate made from waste beverage cans. A sensible heat storage arrangement using gravels was incorporated inside the SAC, extending the operational duration beyond solar radiation h. The results revealed a significant reduction in the drying time of *Curcuma amada* when storage was implemented. The experiments led to the following conclusions:

- *Curcuma amada*, with its original 87.4 % MC, reached an equilibrium moisture level of 4.4 % in just 8 h in SDCWS. In comparison, SDCWOS took 26 h to attain the same MC. In the evaluation of drying kinetics, out of the eleven models chosen, Midilli and Kucuk model emerged as the most suitable fit for both the experiments.
- The observations indicated that a larger portion of the energy derived from the SAC was effectively utilized. With the decline of solar radiation, SAC reached its peak efficiency (91.55 %) when functioning in the SDCWS mode. Due to energy storage, the exit air temperature of the SDCWS mode remained elevated even after sunlight h, whereas for the SDCWOS mode, it decreased as solar radiation decreased over time. The solar dryer demonstrated an average efficiency of 21.88 % for the

SDCWOS and 29.63 % for the SDCWS. The higher average efficiency of the SDCWS can be attributed to its consideration of the total energy utilization due to storage in the system.

- The average exergy efficiencies were 54.50 % and 69.13 % for SDCWOS and SDCWS, respectively. During this study, it was noted that the dryer exhibited elevated exergy efficiencies as the drying periods ended. The exergetic sustainability indicators such as IP and WER and SI had average value of 20.71 W, 0.37, 2.68 for SDCWOS and 15.23 W, 0.31, 3.90 for SDCWS, respectively.
- The samples dried in SDCWS exhibited higher TPC and TFC values compared to those dried under SDCWOS. Upon quality analysis, it is evident that products dried using SDCWS are superior in preserving the original color and texture compared to SDCWOS.
- Economic evaluation was conducted to assess the economic viability of the SDCWS compared to the SDCWOS. This evaluation considered life cycle costs and payback periods. The payback periods were 1.7 years and 0.47 years for SDCWOS and SDCWS, respectively, for the corresponding capital costs (construction costs) of the dryers, which were 22,000 INR and 23,000 INR.